Ceramics International 43 (2017) 17229–17232

Contents lists available at ScienceDirect

Ceramics International

journal homepage: www.elsevier.com/locate/ceramint

Short communication

Low temperature fired $Ln_2Zr_3(MoO_4)_9$ (Ln=Sm, Nd) microwave dielectric ceramics

Weiqiong Liu, Ruzhong Zuo*

Institute of Electro Ceramics & Devices, School of Materials Science and Engineering, Hefei University of Technology, Hefei 230009, PR China

ARTICLE INFO

Keywords:
$Ln_2Zr_3(MoO_4)_9$
Ceramics
Microwave dielectric properties
LTCC

ABSTRACT

A series of new microwave dielectric ceramics $Ln_2Zr_3(MoO_4)_9$ (Ln=Sm (SZM), Nd (NZM)) was successfully fabricated by a standard solid-state reaction method. The X-ray diffraction and Rietveld refinement results demonstrate that pure-phase SZM and NZM ceramics belong to the hexagonal system with a space group $R\bar{3}c$. Scanning electron microscopy results reveal dense and homogeneous microstructures of these two ceramics as sintered at their respective optimum sintering temperature. Furthermore, the SZM and NZM ceramics sintered at 875 °C for 4 h and 850 °C for 4 h possess excellent microwave dielectric properties of dielectric permittivity $\varepsilon_r \sim 11.0$, quality factor Qxf ~ 74,012 GHz (10.6 GHz), and temperature coefficient of resonance frequency $\tau_f \sim -45.3$ ppm/°C, and $\varepsilon_r \sim 10.8$, Qxf ~ 58,942 GHz (10.5 GHz), and $\tau_f \sim -40.9$ ppm/°C, respectively. These experimental results show great potentials for applications of low temperature co-fired ceramic technology.

1. Introduction

With the rapid development of the microwave communication technology, dielectric ceramics with desirable performances are in great demands [1]. Particularly, the low temperature co-fired ceramic (LTCC) technology has played an increasingly important role in the fabrication of modern electronic devices, which would require dielectric ceramics to have a low sintering temperature to be cofirable with Ag, a low permittivity (ε_r) to avoid the signal delay, a high quality factor (Qxf) for better selectivity and a low temperature coefficient of resonant frequency (τ_f) for the frequency stability [2]. In the past decades, a great number of microwave dielectric ceramics such as $Mg_4Nb_2O_9$, Mg_2SiO_4, Zn_2SiO_4 have been developed for their excellent dielectric performances [3–5]. However, the high sintering temperatures have restricted their potential applications in LTCC. The common ways such as adding low-melting additives, chemical processing or using ultra-fine raw materials could solve this problem to a certain degree either at the expense of microwave dielectric properties of the matrix compositions or by increasing the cost significantly. Thus, it is desirable to develop new materials with excellent dielectric properties and inherently low sintering temperatures. In this regard, many Bi_2O_3-, MoO_3-, B_2O_3-, Li_2O- and V_2O_5-based ceramic systems have gained extensive attention [6–11]. Particularly, numerous molybdate ceramics were reported to own excellent microwave dielectric properties and ultra-low sintering temperatures. For examples, $Ag_2Mo_2O_7$ and $Ag_6Mo_{10}O_{33}$ ceramics sintered at 460 °C for 4 h and 500 °C for 4 h possess good microwave dielectric properties of $\varepsilon_r \sim 13.3$, Qxf ~ 25,300 GHz, $\tau_f \sim -142$ ppm/°C and $\varepsilon_r \sim 14.0$, Qxf ~ 8500 GHz and $\tau_f \sim -50$ ppm/°C, respectively [12]. $Na_2Zn_5(MoO_4)_6$ ceramics sintered at 590 °C for 1 h present good microwave dielectric properties of $\varepsilon_r \sim 8.1$ Qxf ~ 35,800 GHz and $\tau_f \sim -95$ ppm/°C [13]. All these attempts would further stimulate us to search for new Mo-based ceramic systems for meeting the demands of LTCC technology.

$Ln_2Zr_3(MoO_4)_9$ (Ln=Sm (SZM), Nd (NZM)) were reported to be good candidates in lighting and display for their desirable spectroscopy, high efficiency, long lifetime, and environment-friendly characteristics [14,15]. Both of them crystallize in a hexagonal system with space group of $R\bar{3}c$ including vertices shared LnO_9, ZrO_6 and MoO_4 polyhedra. Particularly, they can be synthesized at low temperatures of < 900 °C, thus prompting our interests in their microwave dielectric properties. In this work, the SZM and NZM ceramics were prepared by a conventional mixed-oxide route. The crystal structure, sintering behavior, microstructure and microwave dielectric properties were systematically studied for the first time.

2. Experimental procedure

The SZM and NZM ceramics were prepared using high-purity starting powders of analytic-grade Sm_2O_3, Nd_2O_3, ZrO_2 and MoO_3. The raw materials were weighed in stoichiometric amounts and then ball-milled for 4 h using zirconia balls and alcohol as the medium on a planetary milling machine. The resulting slurries were then rapidly

* Corresponding author.
E-mail address: rzzuo@hotmail.com (R. Zuo).

http://dx.doi.org/10.1016/j.ceramint.2017.09.083
Received 30 July 2017; Received in revised form 12 September 2017; Accepted 12 September 2017
Available online 14 September 2017

dried and calcined at 680 °C for 8 h in air. The calcined powders were re-milled for 6 h and then mixed together with 5 wt% PVA as a binder. The granulated powders were subsequently pressed into cylinders with dimensions of 10 mm in diameter and 7–8 mm in height. The specimens were first heated at 550 °C in air for 4 h to remove the organic binder, and then sintered at 800–900 °C for 4 h.

The crystal structure of the fired ceramics was identified via an X-ray diffractometer (XRD, D/Max2500V, Rigaku, Japan) using Cu Kα radiation. The structural parameters were obtained from the Rietveld refinement of the XRD data using the GSAS-EXPGUI program. The bulk densities of the sintered ceramics were measured by the Archimedes method. The microstructure of the specimens was observed using a field-emission scanning electron microscope (FE-SEM; SU8020, JEOL, Tokyo, Japan). Microwave dielectric properties of the sintered ceramics were measured using a network analyzer (N5230C, Agilent, Palo Alto, CA) and a temperature chamber (GDW-100, Saiweisi, Changzhou, China). The τ_f values of the samples were measured in the temperature range of 20–80 °C and calculated by the following equation:

$$\tau_f = \frac{f_2 - f_1}{f_1(T_2 - T_1)} \quad (1)$$

where f_1 and f_2 represent the resonant frequencies at T_1 and T_2, respectively.

3. Results and discussion

Fig. 1 presents the XRD patterns of SZM and NZM ceramics sintered at 875 °C and 850 °C for 4 h, respectively. All the diffraction peaks matched well with the standard pattern of SZM (JCPDS no. 52-0639) and no secondary phase was detected, indicating the formation of pure-phase ceramics of a hexagonal structure with space group $R\bar{3}c$. Because of the structural similarity, the diffraction patterns of SZM and NZM samples look similar and match with each other. To understand their structures in detail, Rietveld refinements based on XRD data were carried out by using GSAS software, in which a structural model of NZM was used. The refined plot of $Sm_2Zr_3(MoO_4)_9$ sintered at 875 °C was selected as a representative, as shown in Fig. 2. The unit cell volume and reliability factors of R_{wp}, R_p, and χ^2 values for all studied samples after the Rietveld refinement are listed in Table 1. The R_{wp}, R_p, and χ^2 values were found to be in the range of 6.2–7.6%, 5.4–6.0%, and 1.7–2.0, respectively, indicating that the structural model is valid and the refinement result is reliable. The lattice parameters are a = b = 9.7871(2) Å, c = 58.180(2) Å for SZM sintered at 875 °C for 4 h and a = b = 9.8042(2) Å, c = 58.508(2) Å for NZM sintered at 850 °C for 4 h, respectively. Moreover, the SEM micrographs on the fracture surface of SZM and NZM ceramics sintered at 875 °C and 850 °C for 4 h, respectively, are shown in Fig. 3. It is obvious that these two samples

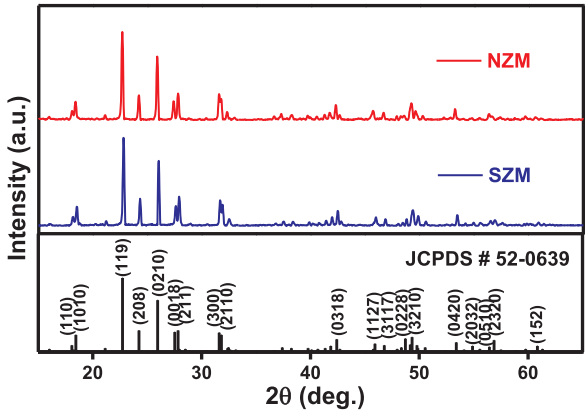

Fig. 1. XRD patterns of SZM and NZM ceramics sintered at their respective optimal sintering temperatures for 4 h.

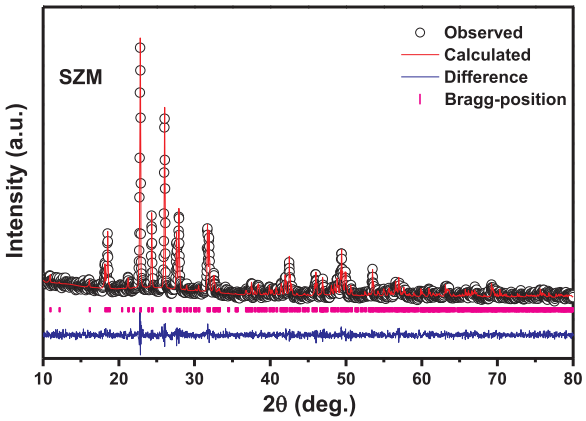

Fig. 2. The Rietveld refinement plot of the SZM ceramic sintered at 875 °C for 4 h.

Table 1
Refined unit cell volume, reliability factors and good-of-fit indicator of $Ln_2Zr_3(MoO_4)_9$ (Ln = Sm, Nd) ceramics at different sintering temperatures.

Compounds	S.T (°C)	Unit cell volume (Å^3)	R_{wp} (%)	R_p (%)	χ^2
$Sm_2Zr_3(MoO_4)_9$	800	4832.1	7.54	5.94	1.94
	825	4831.6	7.28	5.72	2.01
	850	4830.0	7.21	5.73	1.93
	875	4826.3	6.28	5.60	1.90
	900	4826.4	7.34	5.77	2.02
$Nd_2Zr_3(MoO_4)_9$	775	4879.3	7.42	5.60	2.05
	800	4873.5	6.88	5.45	1.78
	825	4872.3	6.86	5.41	1.74
	850	4870.5	7.07	5.65	1.93
	875	4871.0	7.08	5.63	1.88

S.T: sintering temperature; R_{wp}: the reliability factor of weighted patterns; R_p: the reliability factor of patterns; χ^2: goodness-of-fit indicator = $(R_{wp}/R_{exp})^2$.

could be well densified at relatively low temperatures and exhibited dense and uniform microstructure with an average grain size of ~ 1.2 μm.

Fig. 4 shows the variation of relative density and ε_r of SZM and NZM ceramics as a function of sintering temperature. With an increase of sintering temperature, the relative density firstly increased to their respective maximum values, and then decreased slightly with further increasing sintering temperature (see Fig. 4(a)). ε_r also increased to the maximum value of ~ 11.0 at 875 °C for SZM and ~ 10.8 at 850 °C for NZM, and decreased afterwards with increasing sintering temperature. The same variation in ε_r and relative density with sintering temperature obviously indicates that density should be one of the primary affecting factors for ε_r in currently studied ceramics. In order to eliminate the influence of porosity on ε_r, the Bosman and Having's correction was applied to amend the ε_r values of the samples, as expressed by the following equation [16]:

$$\varepsilon_{corr} = \varepsilon_m(1 + 1.5p) \quad (2)$$

where p is the fractional porosity, ε_{corr} and ε_m are the corrected and measured values of the permittivity, respectively. The variation of ε_{corr} as a function of sintering temperature is also shown in Fig. 4(b). As expected, the ε_{corr} values were almost identical in the whole sintering temperature range, but slightly higher than the corresponding ε_m values. The ε_{corr} values of ~ 11.5 and ~ 11.2 were very close to the ε_m values for the SZM ceramic sintered at 875 °C for 4 h and the NZM ceramic sintered at 850 °C for 4 h.

The Qxf values of SZM and NZM ceramics at different sintering temperatures for 4 h are presented in Fig. 5(a). In general, the dielectric loss can be divided into extrinsic loss and intrinsic loss. The extrinsic loss is mainly caused by density, secondary phase, grain size and lattice defects, while the intrinsic loss is mainly caused by structure

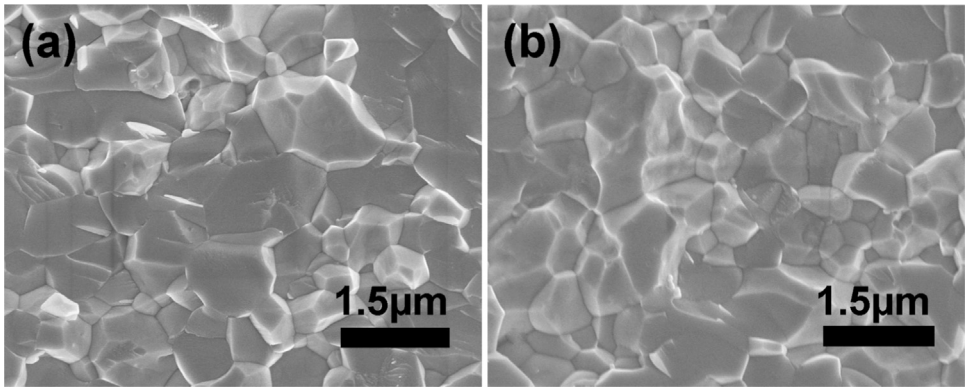

Fig. 3. SEM images of SZM and NZM ceramics sintered at (a) 875 °C and (b) 850 °C for 4 h, respectively.

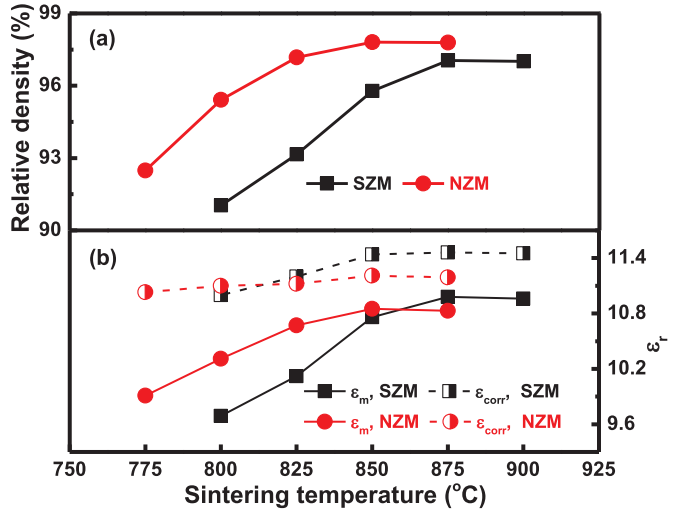

Fig. 4. The variation of (a) relative density and (b) permittivity of SZM and NZM ceramics as a function of sintering temperature.

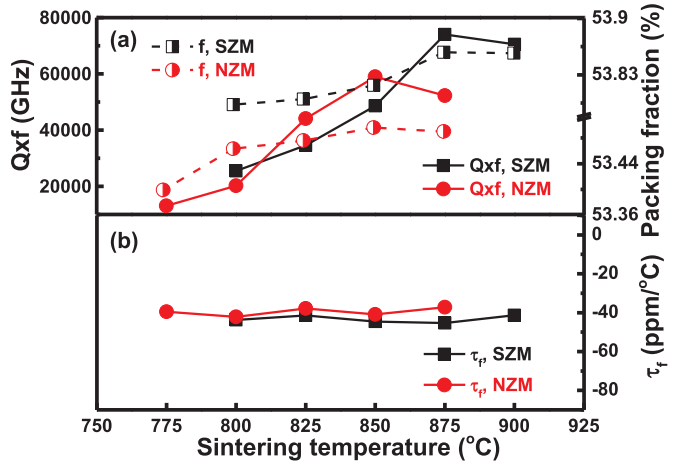

Fig. 5. The variation of (a) Qxf and packing fraction, and (b) τ_f for SZM and NZM ceramics as a function of sintering temperature.

characteristics. The structure characteristics can be evaluated by packing fraction (f) defined by the summation of the volume of packed ions (V_{PI}) over the volume of a primitive unit cell (V_{PUC}). It can be expressed by the following equation [17]:

$$f(\%) = \frac{V_{PI}}{V_{PUC}} \times Z \quad (3)$$

where Z is the number of molecule per unit cell. According to the obtained unit cell volumes at different sintering temperatures in Table 1, the calculated packing fraction of SZM and NZM ceramics is also presented in Fig. 5(a). It can be seen that the variation of Qxf as a function of sintering temperature is consistent with that of relative density and packing fraction, meaning a close dependence of Qxf value on density and packing fraction. The increase in packing fraction means a decreased vibration space, which may give rise to a decrease in the anharmonic vibration, thus leading to a higher Q × f value [17,18]. The maximum Qxf values of 74,012 GHz for SZM and 58,942 GHz for NZM can be obtained at 875 °C and 850 °C, respectively. Considering both SZM and NZM possess a high relative density (> 95%), smaller f values for NZM (~ 53.50) than SZM (~ 53.86) should be responsible for the lower Qxf value of NZM. This means the intrinsic factor should play a dominate role in this case. Fig. 5(b) shows the variation of τ_f values of SZM and NZM ceramics at different sintering temperatures. No obvious changes in τ_f values can be found with increasing sintering temperature. The τ_f values of − 45.3 and − 40.9 ppm/°C were achieved in SZM sintered at 875 °C for 4 h and NZM sintered at 850 °C for 4 h, respectively. The similar τ_f values between SZM and NZM may be ascribed to their same structures, as the τ_f mainly depends on the structure.

4. Conclusions

In this work, two novel low-temperature fired microwave dielectric ceramics SZM and NZM were successfully prepared by a conventional solid-state reaction method. Hexagonal $Ln_2Zr_3(MoO_4)_9$ (Ln=Sm, Nd) ceramics with a space group $R\bar{3}c$ could be well densified at relatively low sintering temperatures (< 900 °C). Excellent microwave dielectric properties of ε_r ~ 11.0, Qxf ~ 74,012 GHz (10.6 GHz) and τ_f ~ − 45.3 ppm/°C, and ε_r ~ 10.8, Qxf ~ 58,942 GHz (10.5 GHz), and τ_f ~ − 40.9 ppm/°C were achieved in SZM ceramics sintered at 875 °C for 4 h and NZM ceramics sintered at 850 °C for 4 h, respectively. The inherently low sintering temperature and good microwave dielectric properties would make these two Mo-based dielectric ceramics become promising candidates in LTCC applications.

Acknowledgements

Financial support from the Special Funds for Science and Technology Development of Guangdong Province (Grant no. 2017A010101001) is gratefully acknowledged.

References

[1] M.T. Sebastian, H. Jantunen, Low loss dielectric materials for LTCC applications: a review, Int. Mater. Rev. 53 (2008) 57–90.
[2] M. Valant, D. Suvorov, Chemical compatibility between silver electrodes and low-firing binary-oxide compounds: conceptual study, J. Am. Ceram. Soc. 83 (2000) 2721–2729.
[3] A. Yoshida, H. Ogawa, A. Kan, S. Ishihara, Y. Higashida, Influence of Zn and Ni substitutions for Mg on dielectric properties of $(Mg_{4-x}M_x)(Nb_{2-y}Sb_y)O_9$ (M = Zn and Ni) solid solutions, J. Eur. Ceram. Soc. 24 (2004) 1765–1768.

[4] T. Tsunooka, M. Androu, Y. Higashida, H. Sugiura, H. Ohsato, Effects of TiO_2 on sinterability and dielectric properties of high-Q forsterite ceramics, J. Eur. Ceram. Soc. 23 (2003) 2573–2578.
[5] Y.P. Guo, H. Ohsato, K. Kakimoto, Characterization and dielectric behavior of willemite and TiO_2-doped willemite ceramics at millimeter-wave frequency, J. Eur. Ceram. Soc. 26 (2006) 1827–1830.
[6] D. Zhou, H. Wang, L.X. Pang, C.A. Randall, X. Yao, Bi_2O_3-MoO_3 binary system: an alternative ultralow sintering temperature microwave dielectric, J. Am. Ceram. Soc. 92 (2009) 2242–2246.
[7] U. Došler, M.M. Kržmanc, B. Jančar, D. Suvorov, A high-Q microwave dielectric material based on $Mg_3B_2O_6$, J. Am. Ceram. Soc. 93 (2010) 3788–3792.
[8] Y.P. Liu, Y.N. Wang, Y.M. Li, J.J. Bian, Low temperature sintering and microwave dielectric properties of $LiMBO_3$ (M = Ca, Sr) ceramics, Ceram. Int. 42 (2016) 6475–6479.
[9] L. Fang, H.H. Guo, W.S. Fang, Z.H. Wei, C.C. Li, $BaTa_2V_2O_{11}$: a novel low fired microwave dielectric ceramic, J. Eur. Ceram. Soc. 35 (2015) 3765–3770.
[10] Y. Wang, R.Z. Zuo, C. Zhang, J. Zhang, T.W. Zhang, Low-temperature-fired $ReVO_4$ (Re=La, Ce) microwave dielectric ceramics, J. Am. Ceram. Soc. 98 (2015) 1–4.
[11] H.H. Xi, D. Zhou, B. He, H.D. Xie, Microwave dielectric properties of scheelite structured $PbMoO_4$ ceramic with ultralow sintering temperature, J. Am. Ceram. Soc. 97 (2014) 1375–1378.
[12] G. Zhang, J. Guo, H. Wang, Ultra-low temperature sintering microwave dielectric ceramics based on Ag_2O–MoO_3 binary system, J. Am. Ceram. Soc. 100 (2017) 2604–2611.
[13] J. Dhanya, A.V. Basiluddeen, R. Ratheesh, Synthesis of ultra low temperature sinterable $Na_2Zn_5(MoO_4)_6$ ceramics and the effect of microstructure on microwave dielectric properties, Scr. Mater. 132 (2017) 1–4.
[14] S. Qi, Y. Huang, H. Cheng, H.J. Seo, Luminescence and application of red-emitting phosphors of Eu^{3+}-activated $R_2Zr_3(MoO_4)_9$ (R = La, Sm, Gd), Electron. Mater. Lett. 12 (2016) 171–177.
[15] R.F. Klevtsova, S.F. Solodovnikov, Y.L. Tushinova, B.G. Bazarov, L.A. Glinskaya, Z.G. Bazarova, A new type of mixed framework in the crystal structure of binary molybdate $Nd_2Zr_3(MoO_4)_9$, J. Struct. Chem. 41 (2000) 280–284.
[16] A.J. Bosman, E.E. Havinga, Temperature dependence of dielectric constants of cubic ionic compounds, Phys. Rev. 129 (1963) 1593–1600.
[17] E.S. Kim, B.S. Chun, R. Freer, R.J. Cernik, Effects of packing fraction and bond valence on microwave dielectric properties of $A^{2+}B^{6+}O_4$ (A^{2+}: Ca, Pb, Ba; B^{6+}: Mo, W) Ceramics, J. Eur. Ceram. Soc. 30 (2010) 1731–1736.
[18] J. Zhang, R.Z. Zuo, Y. Cheng, Relationship of the structural phase transition and microwave dielectric properties in $MgZrNb_2O_8$-TiO_2 ceramics, Ceram. Int. 42 (2016) 7681–7689.